Pergamon

Wat. Sci. Tech. Vol. 31, No. 3-4, pp. 37–47, 1995.

0273–1223/95 $9·50 + 0·00

0273-1223(95)00202-2

A KINETIC MODEL FOR DISSOLVED AIR FLOTATION IN WATER AND WASTEWATER TREATMENT

K. Fukushi*, N.Tambo** and Y. Matsui**

**Department of Civil Engineering, Hachinohe Institute of Technology, 88-1 Ohbiraki, Myo, Hachinohe 031, Japan*
***Department of Sanitary and Environmental Engineering, Hokkaido University, N13W8, Sapporo 060, Japan*

ABSTRACT

A kinetic model for DAF is presented. The author's kinetic model consists of the equations for describing a process of bubble-floc collision and attachment in a mixing zone, and a rise velocity of bubble-floc agglomerates in a flotation tank. The attachment process is formulated on a population balance model with bubbles and flocs as a flocculation in a turbulent flow. The rise velocity of bubble-floc agglomerates is formulated with size of flocs and composition of flocs including the floc density function and attached bubble number. The experimental verification was carried out, using a batch flotation tester and a mini-plant with synthetic clay suspension and colored water. The results successfully verify the validity of the model. From a given condition such as floc size and attached bubble number, the rate and extent of removal by DAF can be readily assessed by the model. A single-collector collision model, often discussed in some occasions, seems to be not useful to describe the DAF process.

KEYWORDS

Dissolved air flotation; kinetics; population balance model; bubble-floc collision and attachment; drinking water treatment; coagulation; flocculation.

INTRODUCTION

Dissolved air flotation (DAF) is an effective solid/liquid separation process for low density floc particles, such as algal flocs, color-alum flocs and clay-alum flocs produced from low turbidity water. Figure 1 is a schematic diagram for a DAF process for drinking water treatment. The DAF facilities are composed of the following four steps: (1) coagulation and flocculation prior to flotation, (2) bubble generation, (3) bubble-floc collision and attachment in a mixing zone, (4) rising of bubble-floc agglomerates in a flotation tank.

The goals of this paper are to present an original kinetic model for DAF process which includes all the above-mentioned steps, and to demonstrate a validity of the model with an experimental verification.

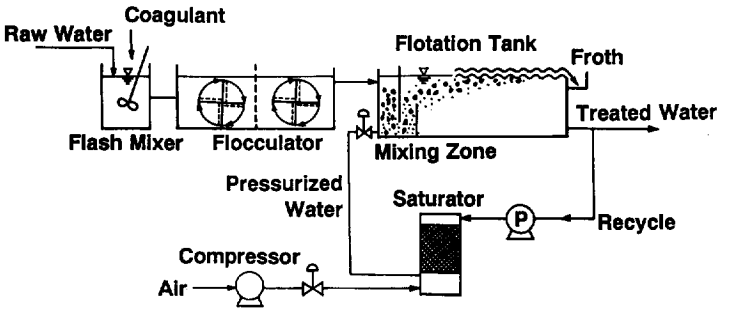

Fig. 1. Schematic diagram of DAF process for drinking water treatment.

FUNDAMENTALS

In recent years, Malley and Edzwald (1991) and Edzwald *et al.* (1990) have proposed a conceptual model for DAF, derived from a single-collector collision theory in a laminar flow condition (SCC model). The authors (Tambo *et al.*, 1985a,b,c, 1986; Fukushi, *et al.*, 1985) however, have already presented a kinetic model, based on the population balance model of bubbles and flocs in a turbulent flow condition (PBT model). As shown in Table 1, many discrepancies are found between both models. The comparison of two models would reveal an essential feature of flotation process.

Table 1. Difference of Model Between Malley and Edzwald and the Authors; Typical Values of Parameters and Concepts

	The authors (1985) (PBT model)	Malley & Edzwald (1990) (SCC model)	
Generated Air Bubbles			
Size range d_a [μm]	10–120 (Ave. 60)	10–100 (Ave. 40)	
Rise velocity w_a [cm/sec]	$w_a=gd_a^2/12\nu$	$w_a=gd_a^2/18\nu$	
Zeta potential [mV]	−150 (at pH 7)	not measured	▲
Pressure P [kPa]	392	345–585	
Recycle ratio r [−]	0.1	0.08	
Concentration n_a [cm^{-3}]	10^4–10^5	10^4–10^5	
Produced Flocs			
Size range d_f [μm]	10^0–10^3	10^0–10^2(10–30 μm is best)	▲
Density ρ_f [g/cm^3]	floc density function	1.01 (assumed)	▲
Suitable mobility [μm/secVcm]	0 − +1 (clay floc) −1 − +1 (color floc)	0.5 or less	▲
Bubble–Floc Collision and Attachment (Agglomeration)			
Collision model	Population balance model	Single-collector collision model	▲
Flow regime	Turbulent flow	Laminar flow	
Mechanism	Locally isotropic turbulence, viscous subrange diffusion	Brownian diffusion, interception, gravity settling	
Attachment mechanism	Electrical-charge interactions (coverage of precipitated coagulant on a floc surface)	Electrical-charge interactions, water layer at floc surface	▲
Rise velocity of agglomerate w_{af} [cm/sec]	According to Eq. 9, 0.1–2.6 (observed)	Nearly equal to w_a, about 0.3	▲

▲; Discrepant items

Generated Air Bubbles

The parameter values of bubbles quite resemble each other. In SCC model, however, the zeta potential of bubbles is unknown. The authors (1985a) found it to be highly negative as -150 mV at neutral pH, using a technique of flotation potential measurement. Collisions between or among air bubbles ineffective for growth due to the high repulsive potential at the surface. This indicates that an electrical-charge interaction between bubbles and flocs is most important for bubble-floc attachment. The attachment will be attainable only at positive sites on a floc surface which consists of a matrix of positive coagulant hydroxides and negative colloidal particles.

Produced Flocs

With respect to produced flocs, there exist many discrepancies with the parameters. The size range of flocs is 10^0-10^2 μm in SCC model, while 10^0-10^3 μm in our PBT model. Edzwald, Malley, *et al.* (1990, 1991, 1992) emphasized that long flocculation is not needed, and flocs should be prepared in a size range of 10-30 μm. The authors agree on the former result, but not the latter. Flocs in general water treatment are actually as large as 10^1-10^3 μm, as shown in Fig. 8. A kinetic model for DAF should be applicable to large flocs in practical processes. Larger flocs have a much higher collision efficiency proportional to a third power of collision radius as mentioned below. Hence, larger flocs should be prepared for effective DAF, to economize capital and running cost. With respect to floc dencisty, SCC model assumes it to be constant, 1.01 g/cm^3. The authors incorporate the accurate floc density function (Tambo and Watanabe, 1976, 1979a) into bubble-floc agglomerates. The function shows that larger flocs have lower density that provides favourable conditions for flotation.

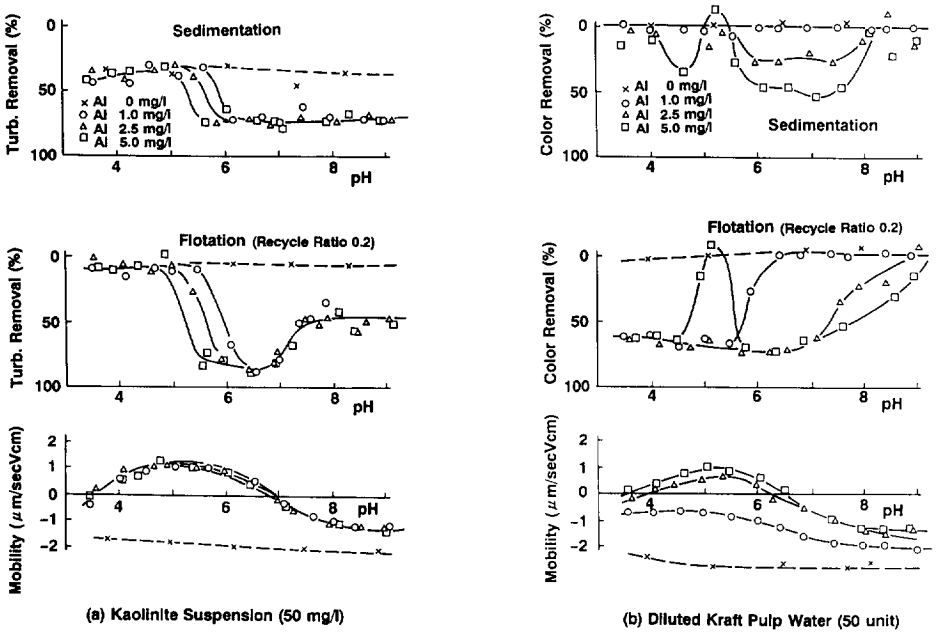

Fig. 2. Relationship between removal and mobility of flocs.

The stability of produced flocs, related to a surface electrical charge, is very important for bubble-floc attachment. The optimal mobility range of flocs for DAF is more accurately studied by the authors (1985a) as shown in Fig. 2. For clay-alum flocs the suitable value for flotation is in a range for 0 to +1 μm/sV cm. In the mobility of zone, both good coagulation-flocculation and attachment of highly negatively charged bubbles to positively charged site of flocs, proceed. For color-alum flocs, the effective mobility zone is

slightly wider such as -1 to +1 μm/sV cm. As colloidal color particles require much higher coagulant dose rate than clay particles, color flocs can have enough positively charged sites even though average mobility is slightly negative.

Bubble-Floc Collision and Attachment

For bubble-floc collision and attachment, there exist significant discrepancies as shown in Fig. 3. The flow regime of SCC model is laminar, in which collision occurs due to Brownian diffusion, interception and gravity settling. Brownian diffusion cannot be dominant for a normal floc and bubble size range for flotation, nor can gravity settling be dominant as mentioned by Malley and Edzwald (1990, 1991) themselves. Thus, only interception is a dominant mechanism in SCC model. The authors consider, however, that interception cannot be dominant in an actual DAF plant. The bubble-floc mixing zone is apparently in a turbulent flow in practice, in which a certain energy dissipation occurs. These conditions are actually observed in our experiments as well as a photograph taken by WRC, U.K. (Melbourne *et al.*, 1977). Interception may play a small role only at the final stage of mixing or in the flotation tank. Before interception takes place, many bubbles can attach to flocs by turbulent transportation within a mixing zone in a very short time, hence bubble concentration in a flotation tank is very low.

Furthermore, even if interception or inertia is dominant, the drag force of collision may cause a difference of velocity between bubbles and flocs in water. The value of difference is nearly equal to the rise velocity of a single bubble (about 0.3 cm/s, 20°C). On SCC model, the rise velocity of bubble-floc agglomerate consequently cannot exceed the value. As shown below in Fig. 9 and 10, however, the agglomerates have a higher velocity (0.1-2.6 cm/s) than the value. This shows that more bubbles can attack onto flocs by a turbulent diffusion rather than a simple interception. On the above mentioned reasons, the authors consider that SCC model is not effectively applicable to describe DAF process, and hence its applicability should be limited to dispersed air flotation or foam separation.

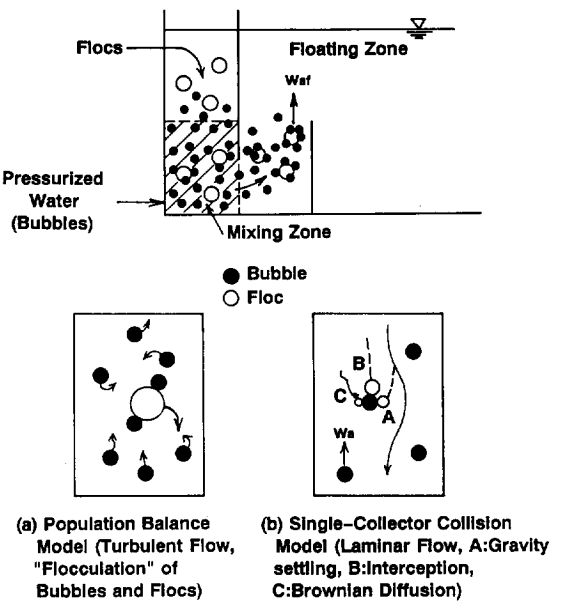

Fig. 3. Concept and mechanism of bubble-floc collison and attachment.

KINETIC MODEL FOR DAF PROCESS

The author's kinetic model consists of the equations for describing the process of bubble-floc collision and attachment (agglomeration) and the rise velocity of bubble-floc agglomerate.

Equation for Describing the Process of Bubble-Floc Collision and Attachment

Formulation is done by counting the number of flocs with attached i bubbles, $n_{f,i}$[cm^{-3}] within an elapsed time of mixing, t [s]. The assumptions for the formulation are as follows. (1) Based on the theory of local isotropic turbulence, in the viscous subrange diffusion (Levich, 1962), agitation intensity in a mixing zone can be experessed by the mean effective energy dissipation rate, ε_o [W/cm^3]. (2) Bubble size is invariable throughout the process, and can be expressed by the mean size (d_a = 60μm) because of its narrow size distribution when comparted with that of flocs, as shown in Figs 7 and 8. (3) Bubbles, once attached onto a floc surface, are held without detachment. (4) There exists a maximum attachable number of bubbles, m_f [-] on a certain size floc, d_f [cm]. (5) Collision-attachment factor, α [-] is calculated from the coverage of cationic precipitated coagulant on a floc surface and the number of attached bubbles, whose initial value when no air bubble is attached, α_o, is ordinarily abour 0.3-0.4. A series of kinetic equations can be written as follows.

$$\frac{d\,n_{f,i}}{d\,t} = \frac{3}{2}\pi\,\beta(\varepsilon_o/\mu)^{1/2} n_a (d_a + d_f)^3 (\alpha_{f,i-1}\cdot n_{f,i-1} - \alpha_{f,i}\cdot n_{f,i}) \qquad (i=1-m_f) \tag{1}$$

$$\frac{d\,n_{f,0}}{d\,t} = \frac{3}{2}\pi\,\beta(\varepsilon_o/\mu)^{1/2} n_a (d_a + d_f)^3 (-\alpha_{f,0}\cdot n_{f,0}) \qquad (i=0) \tag{2}$$

$$\frac{d\,n_a}{d\,t} = -\int_0^{\infty} \{\frac{3}{2}\pi\,\beta(\varepsilon_o/\mu)^{1/2} n_a (d_a + d_f)^3 \sum_{i=0}^{m_f-1} \alpha_{f,i}\cdot n_{f,i}\} dd_f \tag{3}$$

$$m_f = \pi\,\alpha_o (d_f/d_a)^2 \tag{4}$$

$$\alpha_{f,i} = \alpha_{f,0}(1 - i/m_f) = \alpha_o(1 - i/m_f) \tag{5}$$

$$\frac{d\,\bar{i}_f}{d\,t} = \frac{3}{2}\pi\,\beta(\varepsilon_o/\mu)^{1/2} n_a (d_a + d_f)^3\,\alpha_o (1 - \bar{i}_f/m_f) \tag{6}$$

Those equations can be written into a series of normalized dimensionless equations by introducing the following dimensionless variables; F-d_f/d_a (floc size), $N_{F,i} = n_{f,i}/n_f$ (concentration of F-size flocs with i bubbles), $N_a = n_a/n_{ao}$ (free bubble concentration), $N_o = n_{fo}/n_{ao}$ (total floc concentration), $m_f = \alpha_o F^2$ (maximum number of bubbles on a F-size floc), $T = (3/2)\pi\,\beta(\varepsilon_o/\mu)^{1/2} n_{ao} d_a^3\,\alpha_o t$ (normalized mixing time), θ : $d\theta/dT = N_a$ (universal mixing time taking account of a decrease of free bubbles in progress of attachment), where N_f means concentration of f-size flocs, n_a means free bubble concentration, μ means viscosity of water, β equals constant (= $1/15)^{1/2}$), i_f equals averge number of bubbles on a f-size floc, and subscript 'o' means original or initial values.

Although the normalized dimensionless equations are not presented here, those can be solved analytically by way of Laplace transformation methods (Tambo *et al.*, 1985c). The time variation of number of F-size flocs with i bubbles can be calculated by the simple formula as Eq. 7,

$$N_{F,i} = m_F C_i \cdot \exp\{-(1+F)^3\,\theta\} \cdot [\exp\{(1+F)^3\,\theta/m_F\} - 1]^i \qquad (i=0-m_F) \tag{7}$$

where, $m_f C_i$ is the mathematical combination of m_F and i.

The time variation of average bubble number of F-size flocs i_F is written as follows. The use of i_F is a more practical manner to evaluate the progress of air bubble attachment processes with accuracy more than the use of a precise solution of $N_{F,i}$ which counts the distribution.

$$\bar{i}_F = m_F[1 - \exp\{-(1+F)^3 \theta / m_F\}] \tag{8}$$

The relationship between two dimensionless mixing times, T and θ, is described as the following equation,

$$\frac{d\theta}{dT} = 1 - N_o \int m_F[1 - \exp\{-(1+F)^3 \theta / m_F\}]f(F)dF \tag{9}$$

in which floc size distribution function, f(F) is not usually simple, hence a numerical calculation is needed to know the relationship in general. The second term of Eq. 9 denotes a decrease of free bubbled in accordance with the progress of bubble-floc attachment. The universal mixing time, θ can be used for any case in calculating a bubble-floc attachment process. Especially for high concentration suspensions, it is essential to take the decrease of free air bubble concentration with time. In the case of drinking water treatment in practice, suspensions are quite dilute. Therefore, the decrease of free air bubbles with a progress of attachment can be negligible. In this case, the universal mixing time nearly equals to the normalized mixing time, $\theta \Leftrightarrow T$.

Figure 4 shows an example of simulated results after Eq. 7. Assuming the value of α_o, the time variation of number of flocs which attached i bubbles $N_{F,i}$ can be calculated under a given characteristic value or number of bubbles and flocs, and mixing of them.

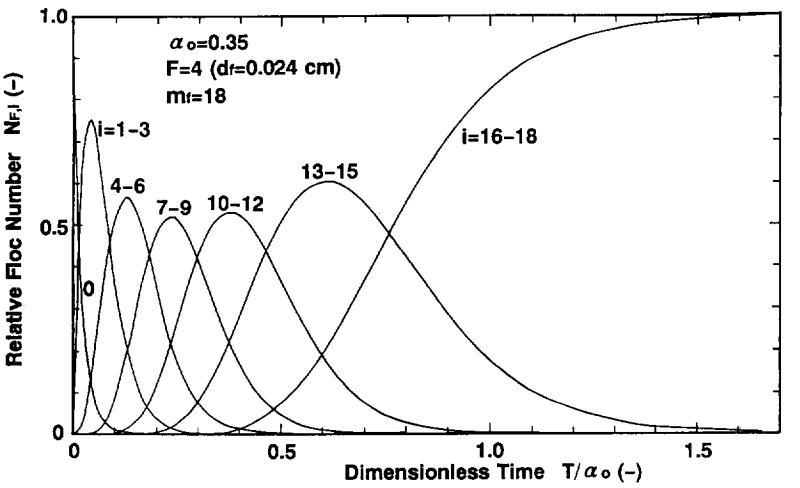

Fig. 4. Simulated result of the time variation of $N_{F,i}$ with mixing time.

Equation for Calculating the Rise Velocity of Bubble-Floc Agglomerate

Introducing a buoyancy of attached bubbles and the change of floc density with the size (floc density function: Tambo and Watanabe, 1979a) into Stoke's equation, the rise velocity W_{af} is calculated by Eq. 10 to 12. The constant k of drag force is approximately estimated by a combination of k values of bubble and floc, using the Rhbczyn'ski-Hadamard formula (Levich, 1962) and the result of Tambo and Watanabe (1979). In the case, k = 16 for bubbles and k = 45 for flocs, respectively.

$$w_{af} = \frac{4g}{3\mu k} \cdot \frac{i(\rho_w - \rho_a) - a(d_f/1)^{-Kp}(d_f/d_a)^3}{i + (d_f/d_a)^3} \cdot d_{af}^2 \tag{10}$$

$$d_{af} = (d_f^3 + i d_a^3)^{1/3} \tag{11}$$

$$k = \frac{16 i d_a^2 + 45 d_f^2}{i d_a^2 + d_f^2} = \frac{16i + 45(d_f/d_a)^2}{i + (d_f/d_a)^2} \tag{12}$$

where, g is the gravity acceleration, ρ_w,ρ_a is the density of water and air respectively, a, K_p is the constants of the floc density function, d_{af} is the diameter of the bubble-floc agglomerate. Practically, the number of attached bubbles, i, is in the order of 10^0 to 10^2, the effective density of a floc is 10^{-3} to 10^{-1} g/cm^3, and the relative dimater of a floc to bubble, d_f/d_a, is 10^0 to 10^1. Therefore, the number of bubbles attached and the floc size deduce a dominant effect on a rise velocity of bubble-floc agglomerates. After all, for given conditions of flocs, bubbles and mixing state, the progress of bubble attachment to flocs can be predicted by Eq. 7 or 8. On the result, the rise velocity distribution of bubble-floc agglomerates can be calculated from Eq. 9, as shown in Fig. 5.

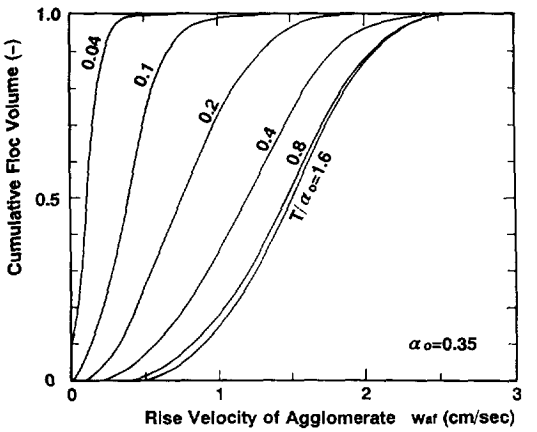

Fig. 5. Simulated result of the rise velocity distribution of agglomerate.

EXPERIMENTAL VERIFICATION OF THE KINETIC MODEL

Experimental Procedures

Experiments were carried out using a batch flotation tester (volume 1.5 l) as shown in Fig. 6 and a continuous flow mini-plant (flow rate of 1 l/min). Tested samples were a synthetic clay suspension and a colored water (diluted kraft pulp black liquor). The size distribution of bubbles and flocs were measured by using a videophotography through a microscope in a specially designed flow cell. Examples of the results are shown in Figs 7 and 8. The rise velocity of bubbles and bubble-floc agglomerates was also measured in the same manner. The constants of floc density function were also evaluated by the above-mentioned videophotography analysis as a = 1.04 x 10^{-4} g/cm^3 and K_p = 1.65.

The concentration of air bubbles was calculated theoretically according to the Henry's law. A case gives the data as na = 7.4 x 10^4 cm^3 at a pressure of 392 kPa with a recycle ratio of 0.1. The effective mean energy dissipation rate ε_o was estimated using the method of Tambo and Hozumi (1979b) on the measurement of maximum floc size in an agitation field, or simply by the calculation of kinetic energy of introduced pressurized water into a mixing zone. The value of ε_o was about 0.006 W/cm^3 for a batch experiment of 0.06 W/cm^3 for a continuous flow.

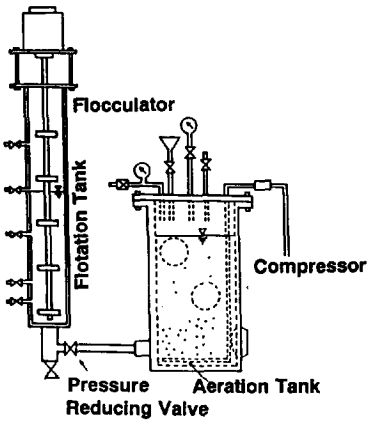

Fig. 6. Schematic diagram of batch flotation tester.

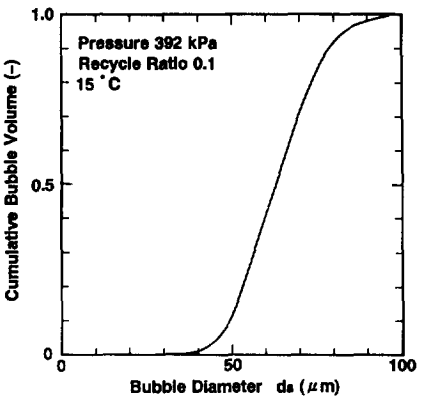

Fig. 7. Size Distribution of bubbles.

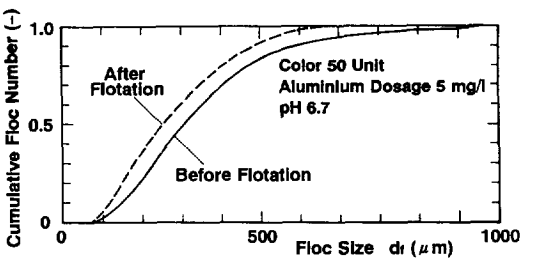

Fig. 8. Size distribution of color flocs.

Estimation of the Initial Collision-Attachment Factor, α_0

Every operation parameter except α_0 was obtained from the above mentioned experiments and theoretical estimation. To set a reasonable value of α_0 and to verify the kinetic model at the same time, a series of calculations to obtain improvement of rise velocity distribution of bubble-floc agglomerates were carried out.

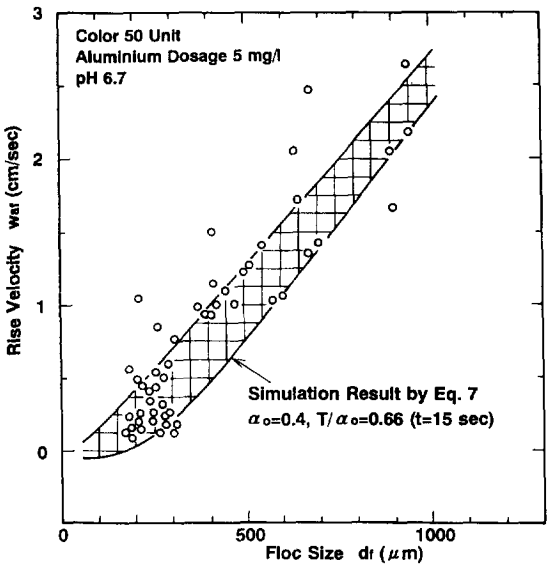

Fig. 9. Rise velocity of bubble-floc agglomerates (color flocs).

Assuming various values of α_0 and comparing the calculated results with the experimental data, the value of α_0-0.4 was considered to be reasonable in the case of color flocs, as shown in Fig. 9. Those data also showed the validity of the above mentioned kinetic model.

The Results of Verification

After the above mentioned analysis, it becomes possible to predict the progress of bubble-floc attachment and improvement of removal rate with an increase of mixing time. Figure 10 presents the improvement of flotability of clay flocs with a various mixing time. In the figure, the experimental result and calculated result show a good fit. The relationship between a mixing time (T or t) and a removal extent of color flocs is also shown in Fig. 11, with various overflow rates in a flotation tank. The experimental result of the simulated resulr show a very good fit.

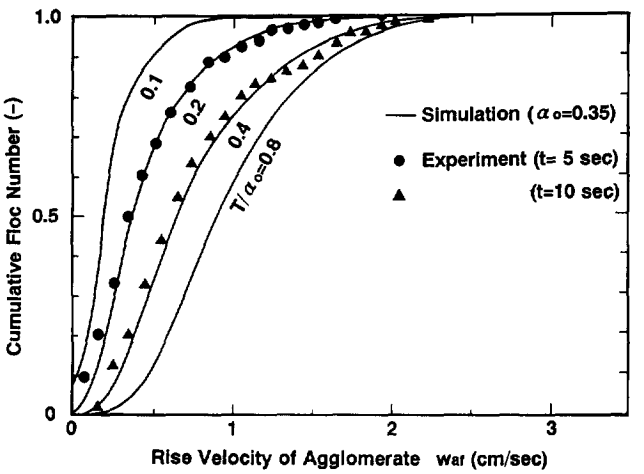

Fig. 10. Improvement of flotability with mixing time (clay flocs).

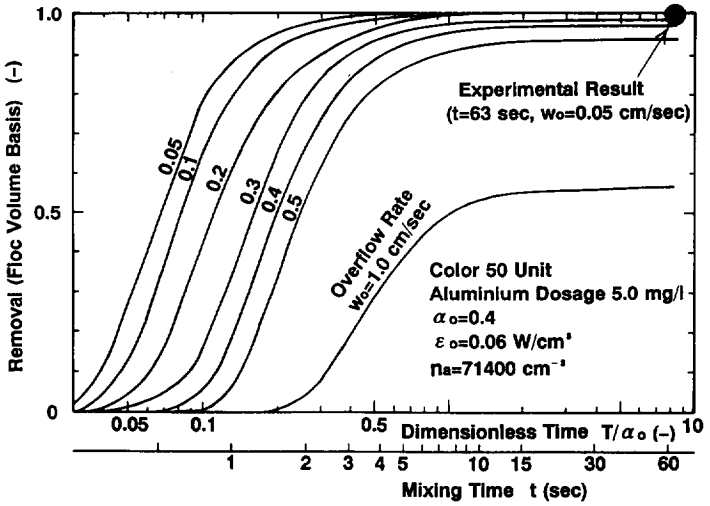

Fig. 11. Relationship between floc removal and mixing time with various overflow rates.

By those calculation, the rate and extent of removal be DAF can be assessed on given characteristic indices of produced flocs, generated bubbles and mixing of the two.

CONCLUSIONS

A kinetic model for DAF in water and wastewater treatment is presented, and is verified by a series of experiments. Conclusions are as follows.

The authors' model can describe the process of bubble-floc collision and attachment in a mixing zone, and the successive improvement of floatability of flocs in a flotation tank. The progress of attachment can be predicted by Eqs. 7 or 8, which are derived from the population balance model of bubbles and flocs. The rise velocity of bubble-floc agglomerates can be calculated from Eq. 9, including the floc density function and the attached bubble number. From a given condition of produced flocs and generated bubbles, the rate and extent of removal by DAF can be readily assessed by the model.

After measuring and estimating fundamental characteristics and parameters of bubbles, flocs and mixing conditions, the verification of the authors' model was carried out. The results successfully showed validity of the model.

By surverying fundamentals of bubbles, floc particles and their agglomeration mechanisms, a single-collector collision model is not effectively applicable to describe the DAF process. Its applicability should be limited to dispersed air flotation or foam separation, where bubbles attack relatively small particles in a laminar flow.

REFERENCES

Edzwald, J. K., Malley, J. P. and Yu, C. (1990). A conceptual model for dissolved air flotation in water treatment. *Water Supply*, **8**, 141-150.

Edzwald, J. K., Walsh, J. P., Kaminski, G. S. and Dunn, H. J. (1992). Flocculation and air requirements for dissolved air flotation. *J. AWWA*, **84**, 92-100.

Fukushi, K., Tambo, N. and Kiyotsuka, M. (1985). An experimental evaluation of kinetic process of dissolved air flotation. *J.JWWA*, **607**, 32-41.

Levich, V. G. (1962). *Physiochemical Hydrodynamics*, Prentice-Hall, pp. 213-434.

Malley, J. P. and Edzwald, J. K. (1991). Concepts for dissolved air flotation treatment of drinking waters. *Aqua*, **40**, 7-17.

Melbourne, J. D., Hyde, R. A., Zabel, T. F. and Maddock, J. E. L. (1977). Summary of 'flotation for water and waste treatment' presented as an audio-visual introduction to the conference. *Papers and Proceedings of WRC Conf. on Flotation for Water and Wastewater*, 1-16.

Tambo, N. and Watanabe, Y. (1976). A study on aluminium floc denisty–1. *J.JWWA*, **379**, 2-10.

Tambo, N. and Watanabe, Y. (1979a). Physical characteristics of flocs–I. The floc density function and aluminium floc. *Wat. Res.*, **13**, 409-419.

Tambo, N. and Hozumi, H. (1979b). Physical characteristics of flocs–II. Strength of floc. *Wat. Res.*, **13**, 421-427.

Tambo, N., Igarashi, T. and Kiyotsuka, M. (1985a). An electrophoretic study of air bubble attachment to aluminium clay-color flocs. *J.JWWA*, **604**, 2-6.

Tambo, N. and Fukushi, K. (1985b). A kinetic study of dissolved air flotation. *J.JWWA*, **606**, 22-30.

Tambo, N., Fukushi, K. and Matsui, Y. (1985c). An analysis of air bubble attachment process of dissolved air flotation. *J.JWWA*, **610**, 2-11.

Tambo, N., Matsui, Y. and Fukushi, K. (1986). A kinetic study of dissolved air flotation. *Proc. World Congress III of Chemical Engineering*, II, 200-203.